Toward an Engineering Model for the Aerodynamic Forces Acting on Wind Turbine Blades in Quasisteady Standstill and Blade Installation Situations

Toward an Engineering Model for the Aerodynamic Forces Acting on Wind Turbine Blades in Quasisteady Standstill and Blade Installation Situations

Mac Gaunaa, Joachim Heinz & Witold Skrzypiński

Technical University of Denmark, Dept. Wind Energy, Frederiksborgvej 399, 4000 Roskilde, DK

macg@dtu.dk

Abstract. The crossflow principle is one of the key elements used in engineering models for prediction of the aerodynamic loads on wind turbine blades in standstill or blade installation situations, where the flow direction relative to the wind turbine blade has a component in the direction of the blade span direction. In the present work, the performance of the crossflow principle is assessed on the DTU 10MW reference blade using extensive 3D CFD calculations. Analysis of the computational results shows that there is only a relatively narrow region in which the crossflow principle describes the aerodynamic loading well. In some conditions the deviation of the predicted loadings can be quite significant, having a large influence on for instance the integral aerodynamic moments around the blade centre of mass; which is very important for single blade installation applications. The main features of these deviations, however, have a systematic behaviour on all force components, which in this paper is employed to formulate the first version of an engineering correction method to the crossflow principle applicable for wind turbine blades. The new correction model improves the agreement with CFD results for the key aerodynamic loads in crossflow situations. The general validity of this model for other blade shapes should be investigated in subsequent works.

1. Introduction

Current state-of-the-art lifting equipment used when erecting offshore wind turbine parks typically have the upper limit of the allowable wind velocity window somewhere between 8-12 m/s. This means that when wind velocity is higher than this threshold, the expensive installation equipment is effectively just waiting for the wind to drop. A significant part of the cost of erecting an offshore wind farm is thus linked to this waiting time. For a middle-sized European offshore wind farm the typical cost of waiting for a lower wind speed window is estimated around 15 million euros. Therefore an effort is being made to understand the physics at play better [1-4]. Furthermore, effort is being put into methods for increasing the upper limit of the allowable wind window using better designs and active control [5]. Since the driving force is of an aerodynamic nature, it is important to be able to understand and accurately predict these forces. The previous work of (some of) the authors investigated in Gaunaa et.al. [4] among others the first-order aerodynamic behavior of a single wing in turbulent inflow by adopting the crossflow principle [6-7] neglecting the induced velocities, and assuming the blade to be straight. The agreement between the statistics of the aerodynamic forces from this model was in good agreement with the one obtained with the aeroelastic code HAWC2 [8], which effectively also use the

crossflow principle for handling situations where the flow is not perpendicular to the blade span. One of the assumptions underlying the crossflow principle is that, the object for which we want to investigate the effect of an added spanwise flow-component is two-dimensional. Since this is clearly not the case for objects such as wind turbine blades, it is of great interest to investigate to what extent the forces on a wind turbine blade behave like the crossflow principle predicts. Therefore, the aim of the present work is to analyze an extensive set of data for the blade of the DTU10MW reference turbine [9] predicted with DTU's in-house CFD code Ellipsys3D [10-12] to assess to what extent the crossflow principle predicts the forces correctly, where and how much it fails, and also to propose a first-order correction model to take into account the three-dimensionality of the wing as an add-on to the crossflow model. The analysis of the CFD data and development of an engineering model for the unsteady loads due to vortex-shedding is described in [13].

2. Approach and methods

The in-house CFD code EllipSys3D [10-12] was used to compute time-marching simulations of the DTU10MW blade geometry using Detached Eddy Simulation with the k-ω Shear Stress Transport turbulence model [14]. The structured computational grid had 128 cells in the spanwise direction, 256 cells in the chordwise direction, 192 cells in the direction normal to the blade surface and a height of the first boundary layer cell of approximately $2 \cdot 10^6$ m. Simulations were carried out for five different yaw-angles (-60°, -30 °, 0 °, +30 °, +60 °) at 52 different pitch-angles of the blades subjected to a constant 12 m/s velocity inflow using a time step of 0.0015 s. This dataset of 260 different inflow directions relative to the 3D blade was used in this work to determine the mean parts of both the integral and sectional aerodynamic loading.

Put in a condensed form, the crossflow principle [6-7] states that the aerodynamic forces on a 2D structure act as if the spanwise flow component was absent.

Defining force coefficients analogous to the standard local unyawed lift (C_l) and drag (C_d) coefficients using the part of the inflow vector perpendicular to the span-direction only we get

$$C_{l,cf} = l_{cf}/(0.5\rho V_\infty^2 cos^2\theta) \quad (1)$$

$$C_{d,cf} = d_{cf}/(0.5\rho V_\infty^2 cos^2\theta) \quad (2)$$

Note that V_∞ is the total inflow velocity magnitude and θ is the yaw angle of the inflow relative to the blade section, where zero is when the flow is perpendicular to the spanwise direction, and positive yaw angles signify flow from the tip of the blade. Additionally it should be emphasized that the lift and drag 'in the crossflow sense' are the forces perpendicular to and parallel with the normal flow component of the inflow vector only.

The cross flow principle also makes definition of the angle of attack in the general yawed case straightforward because it is uniquely defined as in the well-known 2D case when omitting the spanwise part of the inflow vector in the yawed case. Therefore, for a straight blade the angle of attack will not change when the velocity in the spanwise direction is changed.

Since the crossflow principle serves as the baseline model for the behaviour in yawed inflow, local indicators of how well this performs for a fixed total inflow velocity will be the crossflow error ratios defined in Eqs. (3)-(5).

$$R_l(s,\alpha,\theta) = \frac{l(\alpha,s,Yaw=\theta)}{l(\alpha,s,Yaw=0)\cdot\cos^2\theta} = \frac{C_{l,cf}(\alpha,s,\theta)}{C_{l,unyawed}(\alpha,s)} \quad (3)$$

$$R_d(s,\alpha,\theta) = \frac{d(s,\alpha,Yaw=\theta)}{d(s,\alpha,Yaw=0)\cdot\cos^2\theta} = \frac{C_{d,cf}(\alpha,s,\theta)}{C_{d,unyawed}(\alpha,s)} \quad (4)$$

$$R_f(s,\alpha,\theta) = \frac{f(\alpha,s,Yaw=\theta)}{f(\alpha,s,Yaw=0)\cdot\cos^2\theta} = \frac{C_{f,cf}(\alpha,s,\theta)}{C_{f,unyawed}(\alpha,s)} \quad (5)$$

l and d are the local crossflow lift and drag forces per span (see [4]) for constant onset flow velocity magnitude, f is the force magnitude $f = \sqrt{l^2 + d^2}$, s is the span-coordinate of the section, α is the angle of attack (defined without the spanwise part of the velocity, see [4]) and θ is the yaw angle of the flow. This way, the ratios defined in Eqs. (3-5) would be unity if the CFD results behaved

exactly like predicted by the crossflow principle. Furthermore, if an engineering model for the crossflow errors in Eqs. (3)-(4) can be found, it will be possible to predict the local loading in yawed flow from the unyawed case:

$$l(s,\alpha,Yaw=\theta) = R_l(s,\alpha,\theta)\cdot l(s,\alpha,Yaw=0)\cdot\cos^2\theta \quad (6)$$

$$d(s,\alpha,Yaw=\theta) = R_d(s,\alpha,\theta)\cdot d(s,\alpha,Yaw=0)\cdot\cos^2\theta \quad (7)$$

Or it its equivalent coefficient form:

$$C_{l,cf}(\alpha,s,\theta) = C_{l,unyawed}(\alpha,s)\cdot R_l(s,\alpha,\theta) \quad (8)$$

$$C_{d,cf}(\alpha,s,\theta) = C_{d,unyawed}(\alpha,s)\cdot R_d(s,\alpha,\theta) \quad (9)$$

3. Layout of the wing

The key parameters of the layout of the 10MW RWT blade [9] is shown in Figure 1 below.

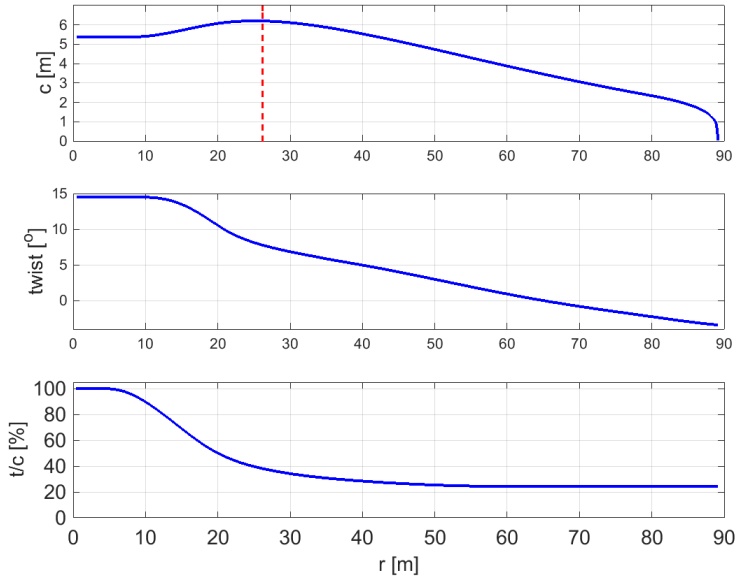

Figure 1: *Key layout parameters for the DTU 10MW RWT blade. Chordlength, c, (upper), twist (middle) and thickness-to-chord ratios, t/c, are shown as function of blade length from the root. The center of gravity at r=26.18 m is indicated with the red dashed line in the upper graph.*

4. Results and Discussion

For the first-order analysis in the current work it is assumed that the velocities induced from the trailed vorticity is negligible. An estimate of the order of magnitude of the induced velocities can be obtained from classic Lifting Line analysis results, where the induced angle of attack is $\alpha_i = C_L/(\pi\cdot AR)$ [rad], where C_L and AR are the integral lift coefficient and aspect ratios, respectively. With a lift coefficient of 1 and an aspect ratio of 10, this correspond to an induced angle of attack of 1.8°, which is smaller than the changes in inflow direction arising from the turbulence in the air in the situations in which wings are mounted ($\sim Tu$ [rad]). Upon neglecting the induced velocities, the sectional lift and drag forces (in the crossflow sense) from the CFD calculations can be found by a simple projection of the sectional forces in the direction perpendicular to and parallel with the part of the farfield inflow vector which is normal to the spanwise direction. The results from the unyawed case, where the inflow is perpendicular to the blade, are shown in the graphs of Figure 2 below.

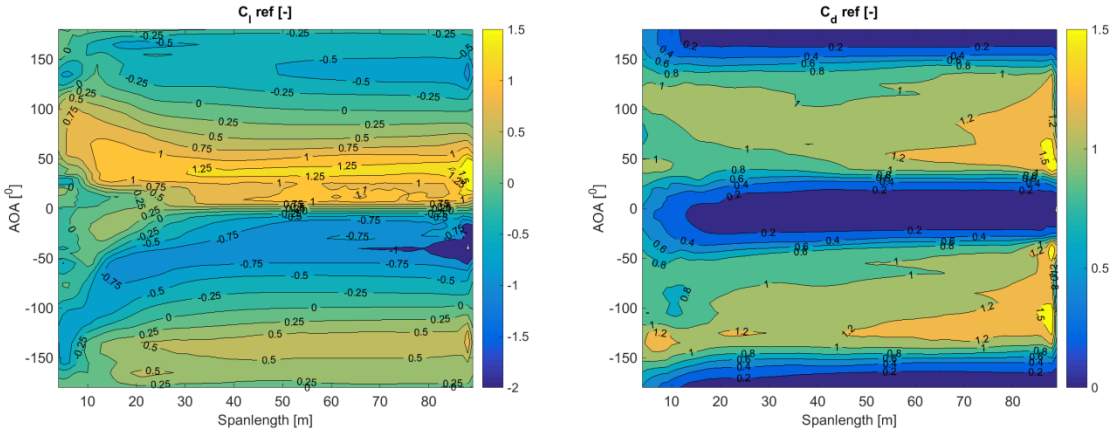

Figure 2: *Sectional lift- (left) and drag coefficients (right) in the unyawed case, $\theta = 0^o$, as function of span position and angle of attack.*

It is observed that the contours of both the lift and drag coefficients in the reference non-yawed inflow case are smooth. Observe also the tendency that the magnitude of the forces and especially the drag coefficient reaches the largest values toward the tip. This is in agreement with what was observed by Sørensen and Michelsen [15] for flat plates and wings at high angles of attack.

The analogous results for also the nonzero angles are shown in Figure A1 in the appendix. From the results it is evident that neither lift-, drag- or force magnitude coefficients are independent of yaw angle. In order to quantify this effect, Figure A2 in the appendix show contour plots of the sectional crossflow correction ratios defined in Eqs. (3)-(5). It is observed that there is only a very small region where the crossflow error ratios are close to unity, which mean that there is only a very small region where the crossflow principle would adequately describe the forces acting on the blade in yawed flow. Another way to show this is to consider the integral moment with respect to the blade center of gravity due to the drag forces. This is shown in Figure 3.

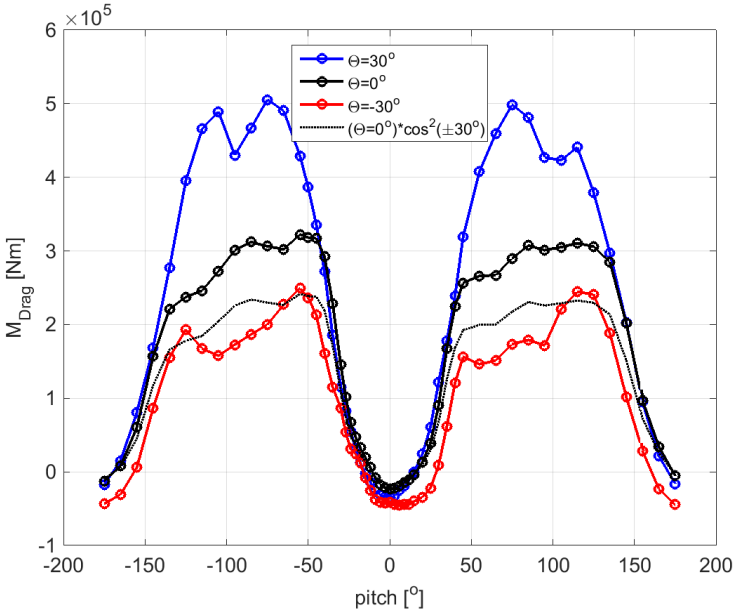

Figure 3: *Integral moment with respect to the blade center of gravity from the aerodynamic drag forces for a wind speed of 10 m/s. The results are shown as a function of blade pitch for yaw angles θ=[-30°, 0°, 30°]. The dotted black curve show what the crossflow principle predicts the moment should have been in the θ=[-30°, 30°] cases.*

If the crossflow principle was correct, it would be expected that all the aerodynamic forces and moments on a wing should scale with $\cos^2\theta$ if the magnitude of the wind was kept constant. This would correspond to a reduction of all forces and moments with a factor of 0.25 for yaw angles of +/- 30°. This is seen to be far from the case in Figure 3, where the aerodynamic torque around the wing center of gravity due to drag forces is shown for yaw angles [-30°, 0 °, +30 °] as a function of pitch angle of the blade. From the crossflow principle it would thus be expected that the blue and red curves should have been identical, and be equal to 75% of the value of the blue curve (shown with the thin black dotted curve). This is clearly not the case. The reason for this is that the aerodynamic forces in the "upwind" part of the blade in the yawed cases have larger values (R_l and R_d) than when they are yawed "downwind".

The region where the crossflow principle describe well the behavior of the aerodynamic loading is seen from Figure A2 to be for the sections with relatively thin airfoils (for r>30 m) for low angles of attack where the flow is probably not stalling (-5°<α<10°). Outside this relatively narrow region it is observed that the error ratios are significantly different from unity. What is also observed from Figure A2 is that, roughly, the shape of the error ratios for lift, drag and total force for a given yaw angle looks similar: $R_l\left(\alpha,\frac{s}{s_{tip}},\theta\right)\approx R_d\left(\alpha,\frac{s}{s_{tip}},\theta\right)\approx R_f\left(\alpha,\frac{s}{s_{tip}},\theta\right)\approx R\left(\alpha,\frac{s}{s_{tip}},\theta\right)$ One explanation for this could be that the extent of a separation zone could be relatively independent of yaw angle, but that the pressure in the separated zone depend on yaw angle and spanwise position along the blade. Another observation that can be drawn from the results in Figure A2 is that the error ratios are relatively symmetric around α=0°: $R(\alpha,\frac{s}{s_{tip}},\theta)\approx R(-\alpha,\frac{s}{s_{tip}},\theta)$. The last observation is the approximate mirroring of the error ratios along the span when the sign of the yaw angle is changed: $R(\alpha,\frac{s}{s_{tip}},\theta)\approx R(\alpha,1-\frac{s}{s_{tip}},-\theta)$. Of course the above observed behavior is very approximate, but it is a good starting point for a first order engineering model of the error ratios. A relatively simple model that has this behavior and resembles the behavior of the error ratios (mainly the total force crossflow error ratio) is presented in Eqs (10)-(11) below.

$$\text{if } \theta>0:\ k=s/s_{tip} \text{ else } k=1-s/s_{tip} \tag{10}$$

$$R(\alpha,k,\theta)=\frac{2}{\pi}\cdot atan\left(40\cdot k\cdot\left(1+1000\cdot\operatorname{sech}\left(\frac{\theta}{2}\right)\right)\right)\cdot\left\{1+|sin\theta|\cdot(k-1/4)\cdot\left(\tfrac{8}{3}\cdot sin^2(\alpha)+\tfrac{2}{3}\cdot|\sin(\alpha)|\cdot sin^2(2\alpha)\right)\right\} \tag{11}$$

Figure A4 in the appendix show contour plots of this approximation for yaw angles θ=[(-60°, -30 °, 0 °, +30 °, +60 °]. This result is then used with Eqs (8)-(9) to model the lift and drag coefficients from the non-yawed case. The result is shown in Figure A3 in the appendix. The comparison with Figure A1 shows that the basic trends are captured. In order to assess better the performance of this first version of a correction model for the crossflow principle, Figure 4 shows key integral aerodynamic loading (lift, drag, lift moment around COG and drag moment around COG) on the DTU 10 MW RWT turbine blade subjected to 10 m/s wind.

It is seen that the results from the model captures the first order of the characteristic behavior for the 30° yaw cases: the magnitudes of integral lift and drag remain fairly constant and the changes to especially the drag moment is rather big. The aim of the approximation of the error ratios was to match the cases with the largest aerodynamic moments, so the performance of the model in the 60° yaw cases is not as good as for the 30° cases, but still the newly proposed model is generally an improvement to the standard crossflow principle.

One valid key question that future works will have to answer is how generally applicable this correction is for other blades (chordlength distribution, twist distribution, thickness distributions, airfoil types, etc.).

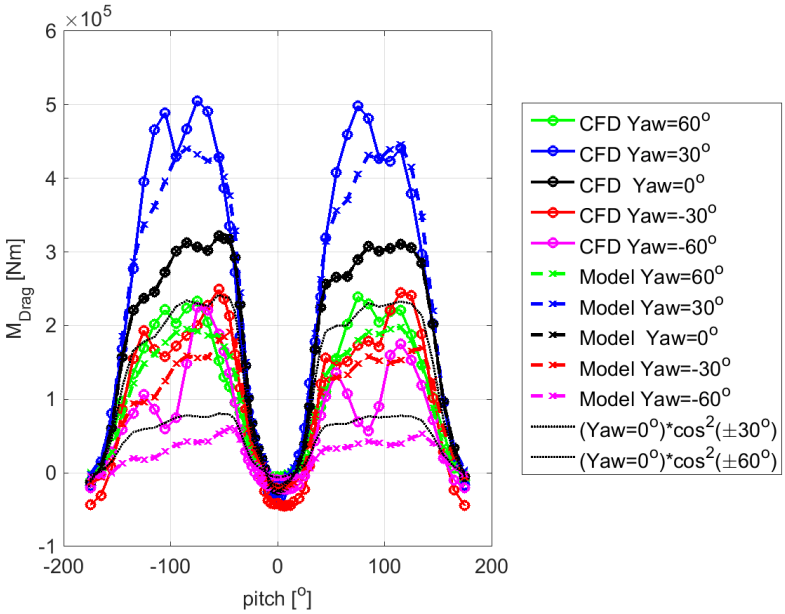

Figure 4: *Integral moment with respect to the blade center of gravity from the aerodynamic drag forces for a wind speed of 10 m/s. Comparison of CFD (full lines) and model (dashed) results. The results are shown as a function of blade pitch for yaw angles θ=[-30°, 0°, 30°]. The thin dotted black curves show what the crossflow principle predicts the moment should have been in the θ=±30° and θ=±60° cases.*

5. Conclusions

CFD simulations were used to investigate the validity of the widely used crossflow principle in the case of flow around a wind turbine wing. It was found that there is only a very limited part of the investigated cases where the crossflow principle can be used to correct the unyawed results to obtain the yawed ones; and in the case of the drag moment around the center of gravity of the blade, the difference between the actual computed values and the ones obtained from combining the unyawed forces with the crossflow principle is very high. This is caused by the aerodynamic forces generally being higher in the "upwind" part of blade and generally lower in the downwind part of the blade. The systematic pattern of the differences was used to formulate a first order engineering correction model to the crossflow principle such that it can be used to determine better the aerodynamic loading in the very complex blade installation and standstill situations. Future works will have to answer how generally applicable the present correction is for blades with different planform/twist/thickness/airfoils.

Acknowledgments

It is gratefully acknowledged that this work was funded by the Danish Energy Agency within the project "Single Blade Installation in high Wind Speeds".

Appendix: Detailed results

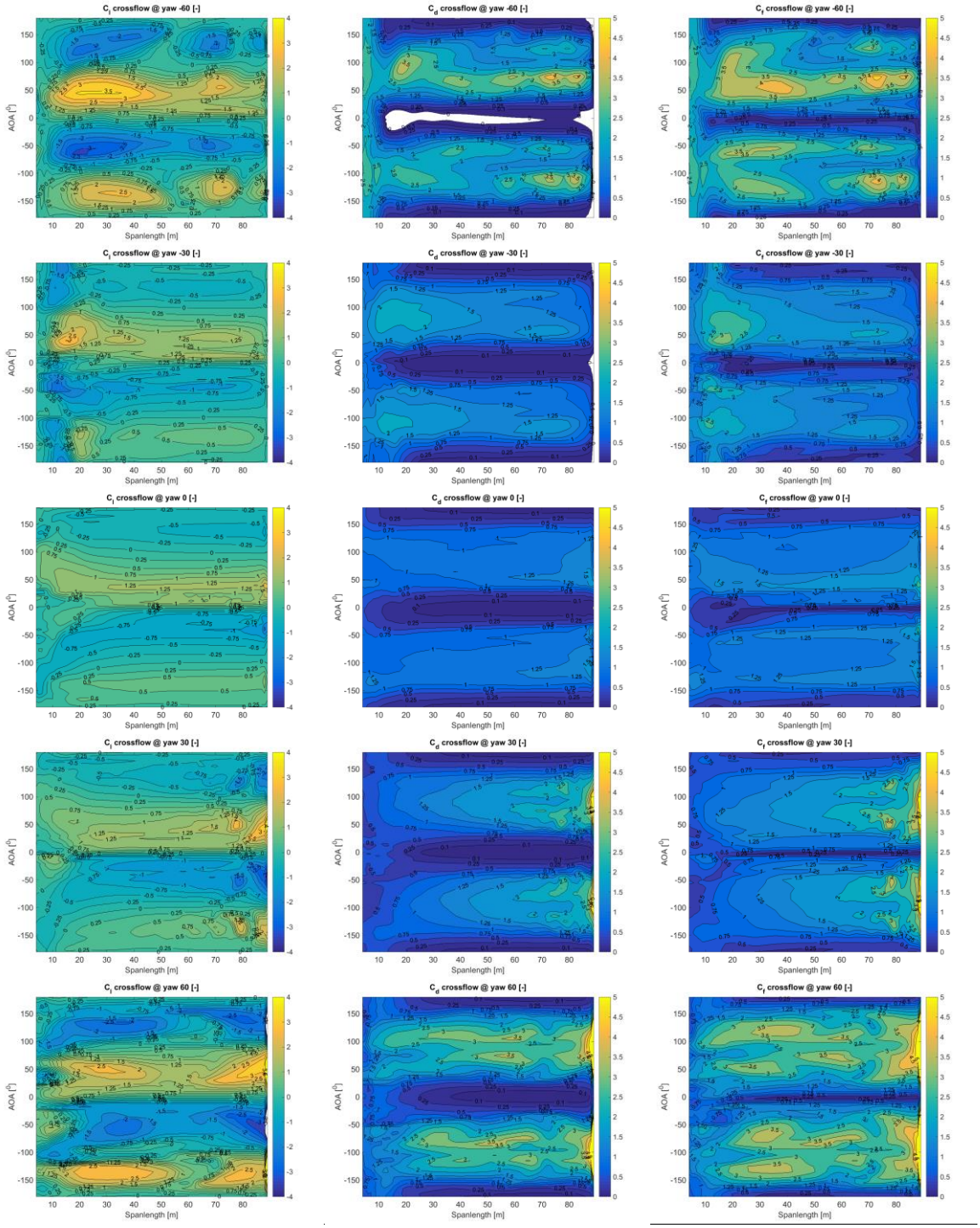

Figure A1: *Contour plots of sectional crossflow lift-(left), drag-(middle) and total force-coefficients (right) for yaw angles -60°(upper),-30°, 0°, 30° and 60°(lower) is shown as function of span position and angle of attack. Note that the coefficients for the unyawed case (0°, middle row) are identical to the ordinary 2D lift, drag and total force coefficients, and are included to make comparison easier.*

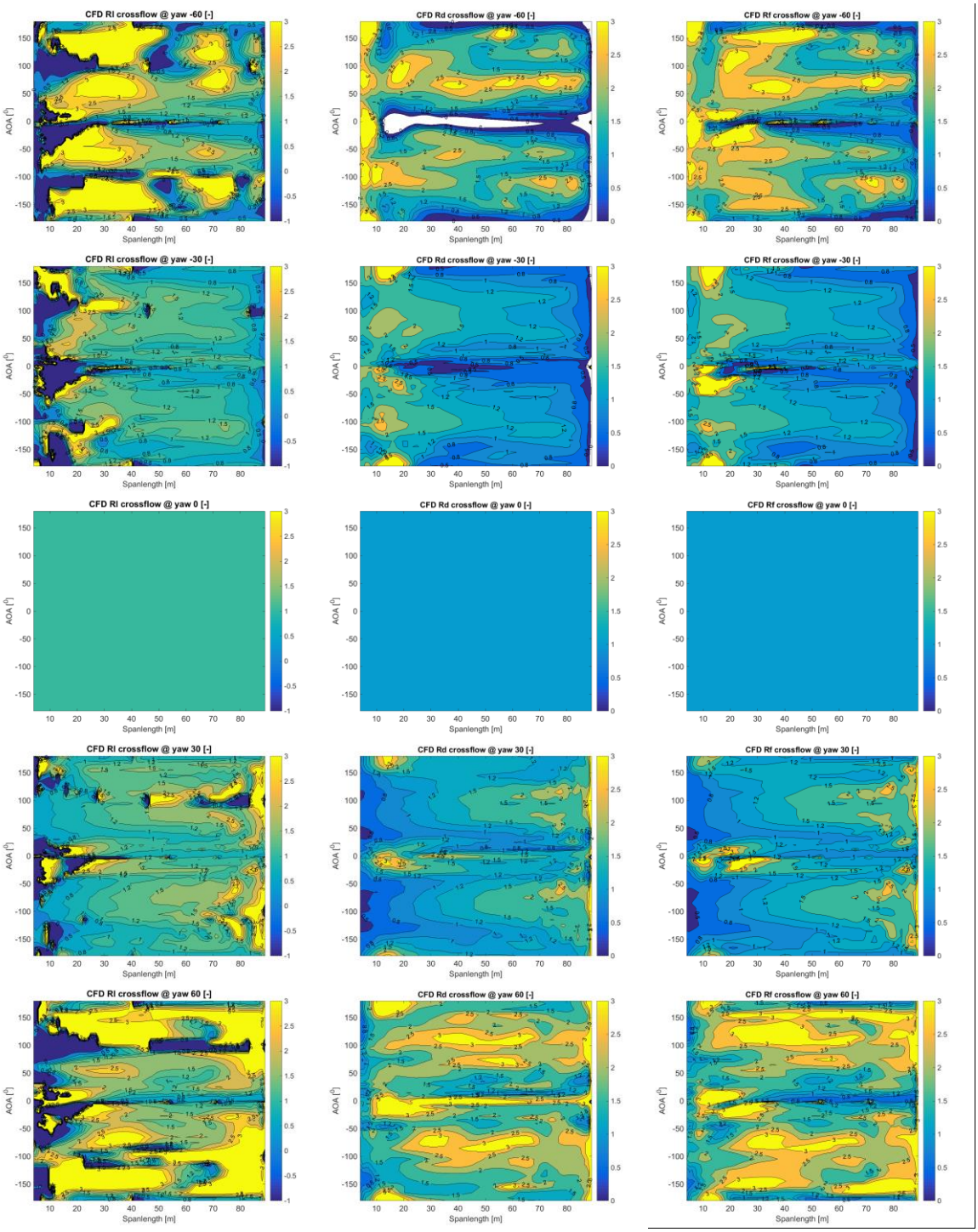

Figure A2: *Contour plots of sectional crossflow correction ratios: R_l(left), R_d (middle) and R_t (right) for yaw angles -60°(upper),-30°, 0°, 30° and 60°(lower) is shown as function of span position and angle of attack. The unyawed case (0°, middle row), where all correction ratios have the value 1, is included to make comparison easier.*

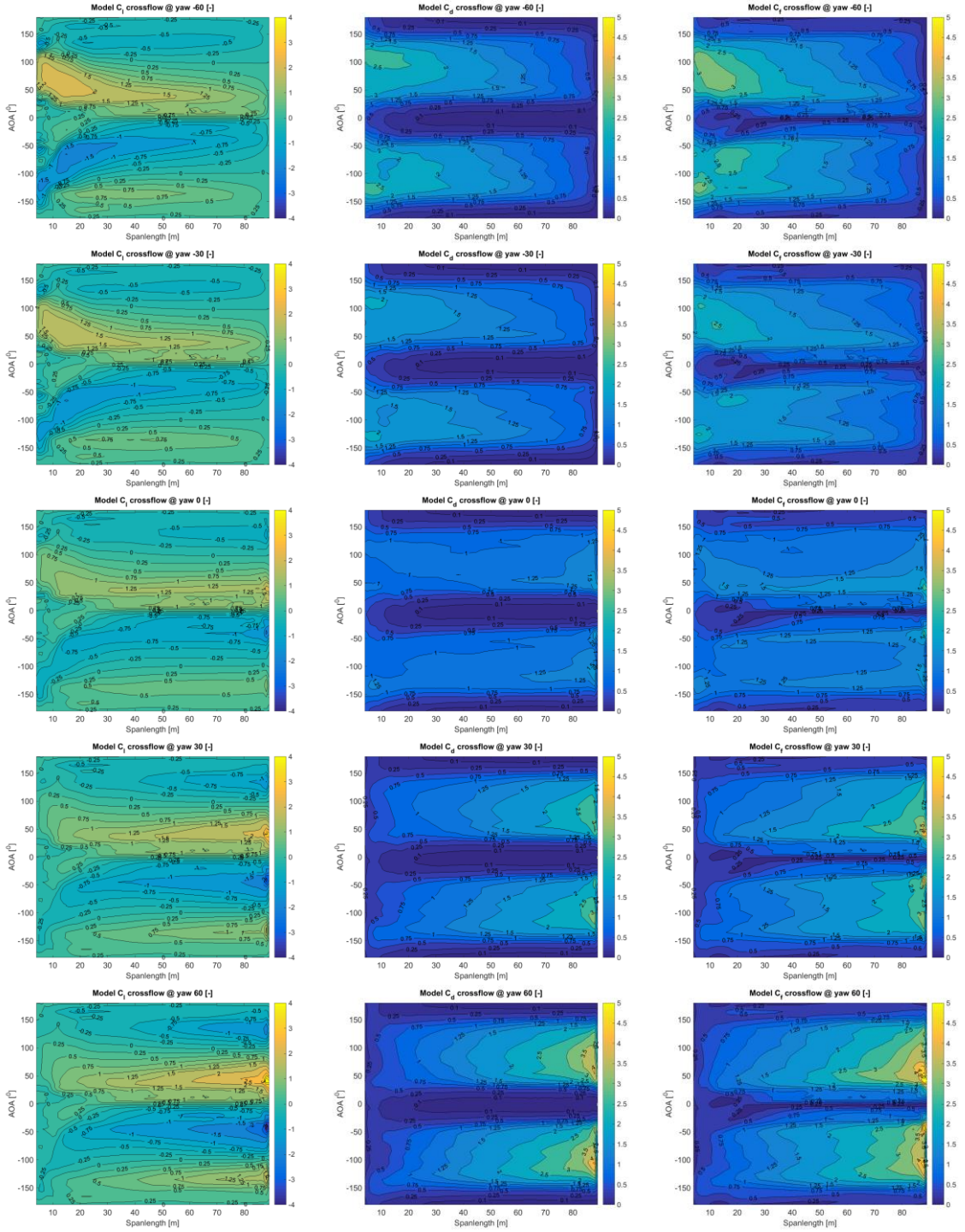

Figure A3: *Contour plots of modeled sectional crossflow lift-(left), drag-(middle) and total force-coefficients (right) for yaw angles -60°(upper),-30°, 0°, 30° and 60°(lower) is shown as function of span position and angle of attack. Note that the coefficients for the unyawed case (0°, middle row) are identical to the ordinary 2D lift, drag and total force coefficients, and are included to make comparison easier.*

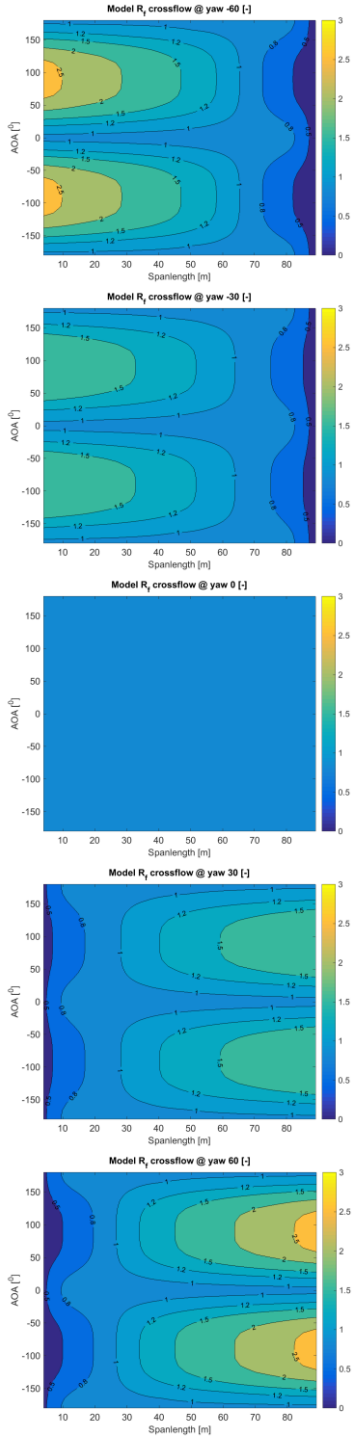

Figure A4: *Contour plots of the results from the model for the sectional crossflow correction ratios for yaw angles -60°(upper),-30°, 0°, 30° and 60°(lower) is shown as function of span position and angle of attack. The unyawed case (0°, middle row) is included to make comparison easier.*

References

[1] Yong Wang, Wei He, and De Tian. Calculation of hoisting forces of the wind turbine rotor based on wind conditions. Renewable Energy, 39(1):323–328, March 2012.
[2] Yong Wang, De Tian, and Wei He. Computation of Hoisting Forces on Wind Turbine Blades Using Computation Fluid Dynamics. Applied Mechanics and Materials, 446-447:452–457, November 2013.
[3] Kuijken, L. Single Blade Installation for Large Wind Turbines in Extreme Wind Conditions. M.Sc. thesis, Denmark Technical University & Technical University of Delft, 2015.
[4] Gaunaa, M., Bergami, L., Guntur, S., & Zahle, F. (2014). First-order aerodynamic and aeroelastic behavior of a single-blade installation setup. Journal of Physics: Conference Series (Online), 524, [012073].
[5] Danish national EUDP Project: Single Blade Installation in High Winds. EUDP 31-I.
[6] Hoerner, S. 1965. Fluid-dynamic drag. Textbook published by the author. Hoerner Fluid Dynamics; Bricktown, New Jersey
[7] Hoerner, S. and Borst, H. 1975. Fluid-dynamic lift. Textbook published by the author. Hoerner Fluid Dynamics; Bricktown, New Jersey
[8] Larsen T. J. 2009 How 2 HAWC2; the user's manual. Tech. Rep. R-1597(EN) Risø National Laboratory. Technical University of Denmark
[9] Christian Bak, Frederik Zahle, Robert Bitsche, Anders Yde, Lars Christian Henriksen, Anand Nata, and Morten Hartvig Hansen. Description of the DTU 10 MW Reference Wind Turbine. Technical Report July, DTU Department of Wind Energy Report I-0092, 2013.
[10] Michelsen, J.A. (1992). Basic3D—a platform for development of multiblock PDE solvers. Report AFM 92-05, Dept. of Fluid Mechanics, Technical University of Denmark, DTU, Denmark, 1992
[11] Michelsen, J.A. (1994). Block structured multigrid solution of 2D and 3D elliptic PDE's. Report AFM 94-06, Dept. of Fluid Mechanics, Technical University of Denmark, DTU, Denmark, 1994.
[12] Sørensen, N.N. (1995). General purpose flow solver applied to flow over hills. PHD Dissertation, Risø-R-827(EN), Risø National Laboratory, Roskilde, Denmark, 1995.
[13] Skrzypiński, W, Gaunaa, M, Heinz, J. Modelling of Vortex-Induced Loading on a Single-Blade Installation Setup, Paper submitted for the Torque 2016 conference
[14] Menter, FR. (1994). Two-equation eddy-viscosity turbulence models for engineering applications, AIAA Journal, Vol. 32, No. 8, pp. 1598-1605
[15] N.N. Sørensen and J.A. Michelsen. Drag Prediction for Blades at High Angle of Attack Using CFD. Journal of Solar Energy Engineering, 126(4):1011, 2004.